High order harmonic generation for study of atomic and molecular dynamics

L. V. Dao,[a] K. B. Dinh, and P. Hannaford
Centre for Atom Optics and Ultrafast Spectroscopy and ARC Centre of Excellence for Coherent X-Ray Science, Swinburne University of Technology, Melbourne, Australia

(Received 4 August 2013; accepted 22 September 2013; published online 3 October 2013)

We present a pump-probe experiment based on the use of a second electrical field to modulate the intensity and the spatial profile of the phase-matched high-order harmonics radiation generated by the first strong driving field. The modification is caused by the variation of the phase-matching condition, e.g., change of electron trajectory and the effect of field gradient forces on the electron that reflect the dynamics of atomic and molecular gases. Atomic argon and molecular oxygen gases are used to demonstrate the feasibility of the technique. © *2013 AIP Publishing LLC*. [http://dx.doi.org/10.1063/1.4824349]

High-order harmonic generation (HHG) provides coherent extreme-ultraviolet radiation and soft x-rays which can be used in time-resolved studies in atomic,[1,2] molecular,[3–5] and solid state systems,[6–8] in extreme ultraviolet interferometry[9] and in coherent diffractive imaging.[10] The theory of HHG can be considered in terms of microscopic and macroscopic aspects. The microscopic treatment is the "single-atom" response or the time-dependent dipole whose Fourier transform is a harmonic spectrum.[11] The process of recombination of the free electron and the parent ion in HHG can be used to study atomic and molecular structural dynamics and opens new directions for studies in atomic and molecular physics.[12,13] The macroscopic phase-matched propagation of the fundamental and harmonic radiation, i.e., the coherent construction of the harmonic field in the macroscopic medium, is reflected in the temporal and spatial profile of the harmonic intensity and plays a major role in experimental aspects but is difficult to include in theoretical calculations. The degree of phase-matching depends on the harmonic order and a number of experimental parameters.

Previous studies of the generation of phase-matched HHG in the near cut-off region using a moveable focusing lens in a semi-infinitive gas cell[14] have shown that the phase change along the focusing beam can be adjusted for phase matching under certain conditions. At the high laser intensities (10^{14}–10^{15} W/cm^2) used for HHG, the electron tunnels through the modified Coulomb barrier at the maximum electric field of the laser cycle, is trapped in a quasi-bound state and then captured into a Rydberg state.[15] The density of these electrons is high and therefore the contribution of excited atoms to the dispersion cannot be neglected; however, the influence of the excited atoms on the phase matching has not been considered in previous studies.

The wave-packet created by the laser field plays a fundamental role in understanding the quantum picture and provides a bridge between the quantum picture and the classical concept of the trajectory of a particle. The motion of the wave-packet reflects the time evolution of a coherent superposition of the system. Useful information regarding the discrimination and visualization of the wave-packet dynamics can be obtained from time-resolved photoelectron imaging because of the sensitivity of the photoelectron angular distribution to the electronic symmetry.[16] The HHG process is a coherent recombination of wave-packets and can be used to study wave-packet properties.[17]

In conventional pump-probe spectroscopy a strong laser pulse is used to excite an atom (or molecule) and the variation of the optical properties following the relaxation or excitation of the atoms (or molecules) is probed by a second delayed pulse. In a HHG experiment, the propagation and phase of the fundamental and harmonic fields depend on the optical properties of the medium and are reflected in the observed harmonic intensity through the so-called phase mismatch factor. A second off-axis delayed pulse can be used to perturb the propagation process or to change the harmonic phase which leads to a variation of the total harmonic intensity and the harmonic beam profile.[18]

In this paper, we report the use of a second, off-axis, long-pulse, laser beam to control the HHG process and show that the dynamics of the excited wave-packet can be studied through the modulation of the HHG intensity and the variation of the beam profile. The experimental approach proposed here shows that the properties and dynamics of the quasi-bound electron wave-packet can be studied and characterised.

A 1 kHz multi-stage, multi-pass, chirped-pulse amplifier system producing up to 10 mJ pulses with a duration of 35 fs and centred at 810 nm is used in our experiment. Details of the HHG setup and detection system have been described elsewhere.[14] The laser beam is split into two beams with an intensity ratio of first beam to second beam of about 4:1. A dispersion medium is added in the path of the second beam to give a pulse duration of ~80fs. The dynamic of ground or ionised electrons can be studied separately when the duration of the controlling (second) pulse is longer than the duration of driving (first) pulse. The extension of the second pulse is short enough for the two pulses to remain phase-locked and the chirp effect can be neglect. The two laser beams are focused to a spot in a gas-filled cell near an exit pinhole at an angle of about 3°. Under these conditions the length of the overlapping region of the two beams is ~2 mm which is smaller than the Rayleigh length (~10 mm). Positive time

[a]Author to whom correspondence should be addressed. Electronic mail: dvlap@swin.edu.au

delay implies that the second beam pulse precedes the first beam pulse.

The total electric field of the q^{th} harmonic E_q emitted along the axis of the fundamental field is given by[19]

$$E_q(L_{med}) = \frac{iq\omega}{\varepsilon_0 c}\rho e^{-L_{med}/2L_{abs}}\int_0^{L_{med}} d_q e^{-z/2L_{abs}} e^{-i(k_q - qk_0)z} dz, \quad (1)$$

where ρ is the gas density, L_{abs} is the absorption length, L_{med} is the interaction length, and d_q is the amplitude of the atomic response. k_q and k_0 are the wave vectors of the q^{th}-harmonic and the fundamental laser field. The phase mismatch $\Delta k = k_q - qk_0$ along the axis of the fundamental laser beam can be expressed as[20]

$$\begin{aligned}\Delta k(z) = &-2\pi P\rho q(1-\eta)[\delta n(\lambda, z) - \delta n(\lambda_q, z)]/\lambda \\ &+ P\rho\eta r_e\lambda(q - 1/q), +(geometric\ term) \\ &+ (dipole\ phase\ term) \\ &+ (dispersion\ of\ highly\ excited\ medium), \end{aligned} \quad (2)$$

where λ is the laser wavelength; P, η, and r_e are the gas pressure, ionization fraction, and classical electron radius, respectively; and $\delta n(\lambda,z)$ and $\delta n(\lambda_q,z)$ are the linear and nonlinear dispersion of the gas at the fundamental and harmonic wavelengths per unit atomic density. The first term (in square brackets) in Eq. (2) is related to the dispersion of the neutral medium, which is negative, and the second term is the plasma dispersion, which is positive. The geometric term is dependent on the configuration of the HHG setup. Electrons which have tunnelled under the interaction of the laser field at the maximum electric field of a laser cycle can return to the atom after one cycle with zero kinetic energy[21] and oscillate with the laser frequency in the next cycle. These electrons can be captured into a Rydberg state after a few optical cycles of the pulses. When a long laser pulse is applied a quasi-bound wave-packet and a Rydberg state with a high density wave-packet are created. We include in Eq. (2) a term due to the dispersion of the highly excited medium to take account of excitation effects. The neutral and plasma dispersions are characterized by refractive indices[22] and depend on laser intensity and the length of the medium along the propagation direction. The dipole phase and the contribution of the highly excited atoms are space-dependent phases and vary along the transversal and longitudinal direction.

When the second beam is absent the pressure, aperture diameter, energy and chirp of the first laser pulse are optimized for maximum total harmonic flux and narrow bandwidth for all available harmonics. The optimised HHG spectrum, which is recorded along the x-axis of the CCD detector, is shown in the inset of Fig. 1(b) for HHG from argon gas. A good beam profile, which is recorded along the y-axis of the CCD, indicates that the phase mismatch is small for a short quantum pathway along the optical axis.[14] The dispersion of the neutral medium is much smaller than the plasma dispersion,[20] so that the release of a few electrons is sufficient to alter the balance of the neutral atom dispersion. The harmonic intensity and spatial profile are sensitive to any change of the phase mismatch factor.

When the second laser field is applied the harmonic intensity varies with the delay time between the two beams because

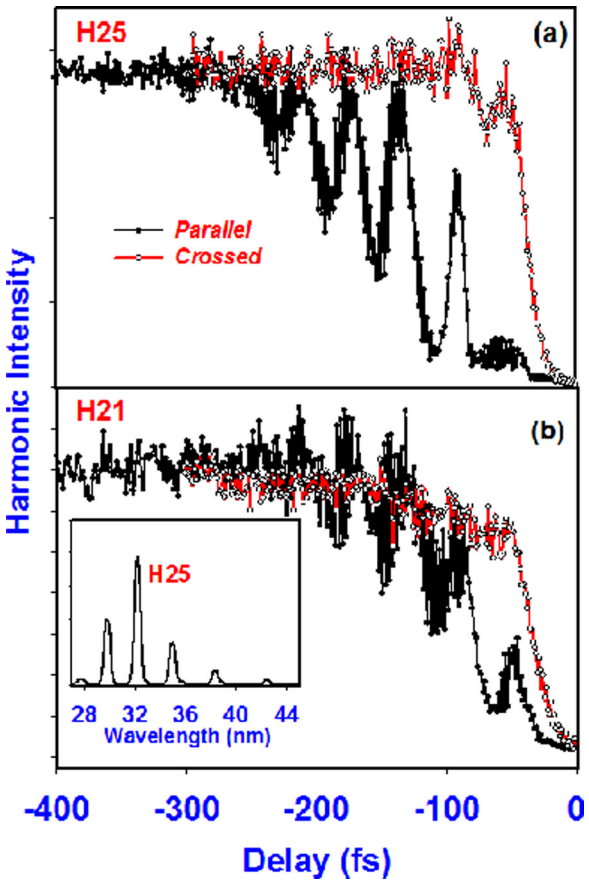

FIG. 1. Modulation of the intensity of harmonics H21 and H25 versus delay time of the second beam for argon gas. The inset shows the phase-matched high-order harmonic spectrum from argon gas.

the phase-mismatch Δk is altered. Similar to the use of a spatial filter to isolate the contribution of different quantum paths,[23] we select the central region along the optical axis to analyse the intensity of the harmonics. Figure 1 shows the variation of intensity with delay time of the second beam for two harmonics: the 25th harmonic (H25–Fig. 1(a)) which has the highest intensity and the 21st harmonic (H21–Fig. 1(b)), when argon gas is used. The intensity of the second pulse is $\sim 3.10^{13}$ W/cm^2. The polarization of the second laser field is set both parallel and crossed to that of the first laser field. Figure 2 shows the intensity of the 21st harmonic (H21–Fig. 2(a)) and the 17th harmonic (H17–Fig. 2(b)) for molecular oxygen versus delay time of the second beam.

When the two laser fields overlap in time (i.e., the delay time is less than the pulse duration $\sim$80 fs) the output harmonic intensity is very low. In our experiment, the intensity of the off-axis second beam is high enough to produce a nonlinear response and to change the trajectory of the free electrons[24] in the overlapping region. A large additional mismatch factor is created in the overlapping region and the minimum of the phase mismatch established by optimization of the first laser field is disrupted.

For a long negative delay ($\tau < -50$ fs) the modulation of the harmonic intensity is very strong for parallel polarizations for delay times up to -300 fs. When a 80 fs hyperbolic secant second pulse is applied the ratio of the first second field strength is $\sim$0.05 and 0.01 at a delay time of -200 fs and -300 fs, respectively. The second field does not change

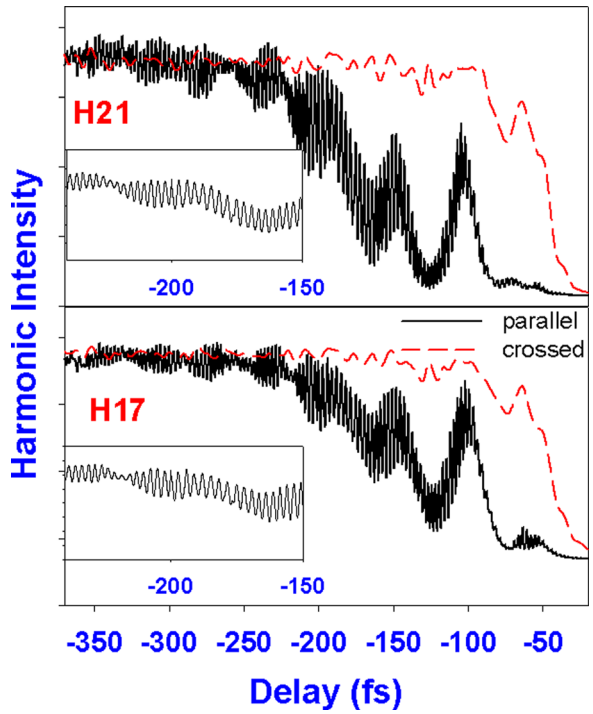

FIG. 2. Modulation of the intensity of harmonics H17 and H21 versus delay time of the second beam for oxygen gas. The inset shows a zoom of the region near the time delay of −200 fs.

the field strength of the first field but it is enough to modify the trajectory of the free electron. It is worth to note that the modulations of the HHG radiation for the positive and negative delay are differently (we don't consider that in this paper). A high modulation frequency, which is the same as the laser frequency, and a low modulation frequency (20–25 THz) can be seen in Figs. 1 and 2. The longer modulation period is ∼40 fs for argon and ∼ 50 fs for molecular oxygen. According to the three step model of HHG, the electrons are most likely produced at the peak of the electric field but they return to the core with zero kinetic energy and are trapped in a quasi-bound state. They are not contributed to HHG emission but their contributions to phase-matching cannot be neglected. The properties of the electrons in these states are not well understood. The second (weak) pulse excites the quasi-bound and high excited wave-packet, which is likely to be a highly excited Rydberg wave-packet, into the ionized continuum. The interaction of the second field with parallel polarization is strong because the quasi-bound and Rydberg states are high dipole states. The free electron wave-packets created by the first laser field, when they interact with the field before or after the maximum, and the other free electron wave-packets created by the second laser field through the ionization of the high-excited wave packet can interfere with each other. We can consider a double-peaked free electron wave-packet originating neither from double ionization nor from single ionization. The ionization of the quasi-bound wave-packet and the interference of the two wave-packets leads to a change of the plasma dispersion. The interaction of the second laser field with the free electrons modifies the trajectory and re-scattering of the electron causes a change in the dipole phase. In the longitudinal direction or in the total harmonic intensity, the contribution of the dipole phase to the phase-mismatch is smaller than that of the plasma dispersion.

Using a strong many cycle pulse (duration ∼30 fs), a quasi-bound electron with very low kinetic energy and a short-lived Rydberg wave-packet are created by the tunnelling of the electron at the maximum electric field of each laser cycle. In the rotating wave approximation, the density of the combined wave-packet during the interaction of the first field can be written as[25]

$$P(t) \sim [\ 1 + \beta \cos \omega_{12} t], \tag{3}$$

where β is the coupling between the two wave-packets and ω_{12} is the frequency splitting of the two states. These wave-packets can be ionized by the second weak laser field to continuum states. The laser electric field used to generate a coherent double-peaked free wave-packet in the continuum state is given by $E(t) = E_1(t) + E_2(t+\tau)$. The additional electrons in the continuum state can be expressed as[26]

$$N_e = [1 + \gamma \cos \omega_l \tau] f_2(\tau) P(\tau), \tag{4}$$

where ω_l is the laser frequency, $f_2(\tau)$ is the intensity envelope of the second laser field, and γ is the transition probability. The intensity envelope of the second laser field is $f_2(\tau) = E_0\,\mathrm{sech}^2(\tau/T_2)$, where T_2 is the pulse duration of the second laser field and N_e is the normalised electron density. These electrons will change the plasma dispersion and the dispersion of the highly excited electrons in the second and fifth terms of Eq. (2) which leads to a change in the phase-mismatch. The phase-mismatch will increase with N_e, and a variation of the HHG intensity scales as $(1-N_e)$. Figure 3 shows the modulation of the harmonic intensity for time delays of around −200 fs for argon. The insets in Fig. 3 show simulations of Eq. (4) for different coupling factors β and γ. The duration of the second pulse is $T_2 = 80$ fs and the frequency $\omega_{12} = 25$ THz (40 fs) corresponding to the splitting of the quasi-bound and Rydberg states. The simulations show a similar variation of the harmonic intensity to that of the experimental observations. The coupling factors are dependent on the harmonic order.

We consider now the transverse phase-mismatch. When an atom or molecule interacts with a strong laser field a phase of the atomic or molecular dipole (atomic phase) φ_{at} is induced. The harmonic intensity is the sum over quantum paths and the phase of each path results from the phase due to the time delay between the electron-ion recombination time and the reference time of the laser period. This phase is given by[18]

$$\varphi_{at} = q\omega t_f - \frac{1}{\hbar}\ S, \tag{5}$$

where S is the quasi-classical action for an electron excited to the continuum at t_i with a canonical momentum p and returning to the origin at t_f. For each quantum path, the action can be approximated by $-t_s U_p$, where $t_s = t_f - t_i$ is the return time and $U_p = E^2/4\omega^2$ is the ponderomotive potential.

The gradient of the atomic phase will create an effective wave-vector $\boldsymbol{K_t(r,z)} = \nabla \varphi_{at}(r,z)$[18] which is proportional to the spatial derivative of the action. In a simple case this

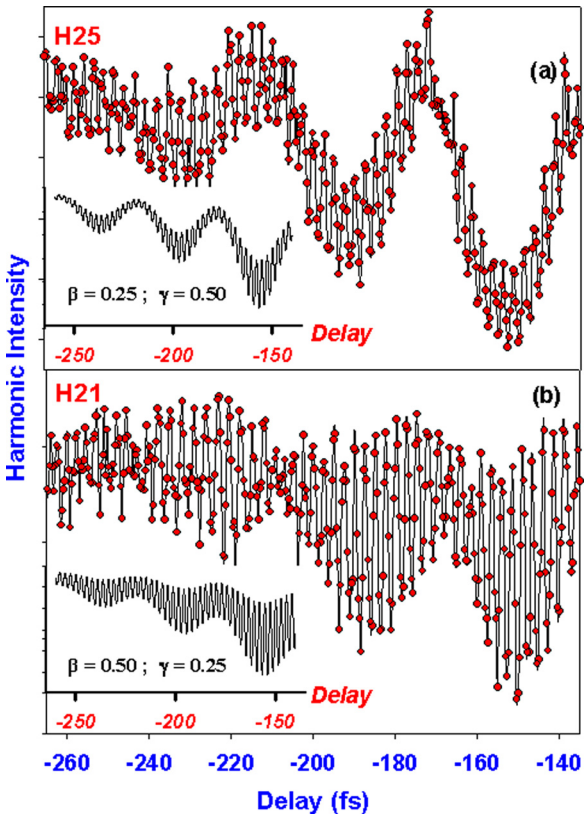

FIG. 3. Modulation of the intensity of harmonics H21 and H25 versus delay time of the second beam around −200 fs for argon gas. The insets show simulations of the phase mismatch caused by ionization of the quasi-bound wave-packet.

phase varies linearly with the laser intensity I: $\varphi_{at} = -\alpha_q I$,[23] where $\alpha_q \approx 1 \times 10^{-14}$ cm^2 W^{-1} and $\approx 25 \times 10^{-14}$ cm^2 W^{-1} for the short and long quantum trajectories, respectively. However, when a second laser field interferes with the free electrons, the return time is altered and the coefficient α_i is changed by an amount dependent on the strength of the second laser field. Because the phase-mismatch of the long trajectory is large the contribution of the long trajectory to the total phase-matched HHG intensity is small. However, the second laser field interferes with the trajectory of the free electron and changes the atomic phase which is reflected in the beam profile of the harmonic in the far-field. This can be used for a direct study of the motion of the electronic wave-packet in the continuum including the dynamics of electron rearrangement prior to recombination.

The insets in Fig. 4 show the beam profile of H21 and H17 for oxygen at around −100 fs where the phase-mismatch is large and the harmonic intensity is low. Within one optical cycle, we observe a shifting of the maximum with delay time away from the axis (for delay ∼ −108 fs) to an asymmetrical annular beam around the optical axis of the driving field (for delay ∼ −109 fs) and then an abrupt change back to on-axis (for delay ∼ −110 fs). When the divergence is a maximum we observe contributions from both off-axis and on-axis radiation. An asymmetrical annular beam (around the optical axis of the generated field) may result when the two fields are aligned off-axis. The momentum gain of a free electron, $\delta \boldsymbol{P}_{\mathbf{elec}} = \hbar \boldsymbol{K}_t$ is transferred to the harmonic photon, and is taken into account in the phase-matching condition.[18] Based

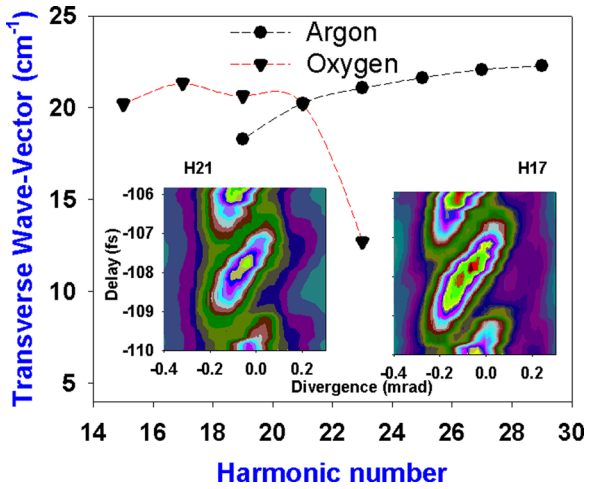

FIG. 4. Maximum of the transverse wave-vector measured by the second beam. The insets show the beam profiles of H21 and H17 for oxygen at around −110 fs.

on momentum conservation of the wave-vector, $\boldsymbol{K_q} = q\boldsymbol{K_0} + \boldsymbol{K_t}$, we can determine the $|\boldsymbol{K_t}|$ for different harmonic orders. While the transverse effective wave-vector and hence the transverse phase exhibits a slight monotonic increase with harmonic order for argon the phase for molecular oxygen changes abruptly for the harmonic at the cut-off as shown in Fig. 4. The changing of the return time (τ_s) involving the second pulse alters the phase front of the harmonic field, which is reflected in the far-field spatial profile.[24] We can expect that the variation of the spatial profile depends on the atomic and molecular structures.

In conclusion, using a long off-axis pulse to modify the phase-matched harmonic intensity and the spatial distribution, the contribution of different electron trajectories can be revealed. We demonstrate that information on the quasi-bound state and the Rydberg state can be obtained from the high-order harmonic generation process. This experimental technique offers the possibility of studying the dynamics of the phase matching of an atom and the molecular structural dynamics with high time and spatial resolution.

[1]M. Gisselbrecht, D. Descamps, C. Lyngå, A. L'Huillier, G. Wahlström, and M. Meyer, Phys. Rev. Lett. **82**, 4607 (1999).
[2]M. Uiberacker, T. Uphues, M. Schultze, A. J. Verhoef, V. Yakovlev, M. F. Kling, J. Rauschenberger, N. M. Kabachnik, H. Schröder, M. Lezius, K. L. Kompa, H. G. Muller, M. J. J. Vrakking, S. Hendel, U. Kleineberg, U. Heinzmann, M. Drescher, and F. Krausz, Nature **446**, 627 (2007).
[3]S. L. Sorensen, O. Björneholm, I. Hjelte, T. Kihlgren, G. Öhrwall, S. Sundin, S. Svensson, S. Buil, D. Descamps, A. L'Huillier, J. Norin, and C. Wahlström, J. Chem. Phys. **112**, 8038 (2000).
[4]E. Gagnon, P. Ranitovic, X. M. Tong, C. L. Cocke, M. M. Murnane, H. C. Kapteyn, and A. S. Sandhu, Science **317**, 1374 (2007).
[5]M. Bauer, C. Lei, K. Read, R. Tobey, J. Gland, M. M. Murnane, and H. C. Kapteyn, Phys. Rev. Lett. **87**, 025501 (2001).
[6]A. L. Cavalieri, N. Müller, T. Uphues, V. S. Yakovlev, A. Baltuška, B. Horvath, B. Schmidt, L. Blümel, R. Holzwarth, S. Hendel, M. Drescher, U. Kleineberg, P. M. Echenique, R. Kienberger, F. Krausz, and U. Heinzmann, Nature **449**, 1029 (2007).
[7]L. Miaja-Avila, C. Lei, M. Aeschlimann, J. L. Gland, M. M. Murnane, H. C. Kapteyn, and G. Saathoff, Phys. Rev. Lett. **97**, 113604 (2006).
[8]M. Schnürer, Ch. Streli, P. Wobrauschek, M. Hentschel, R. Kienberger, Ch. Spielmann, and F. Krausz, Phys. Rev. Lett. **85**, 3392 (2000).
[9]D. Descamps, C. Lyng, J. Norin, A. L'Huillier, C.-G. Wahlstrom, J.-F. Hergott, H. Merdji, P. Salieres, M. Bellini, and T. W. Hänsch, Opt. Lett. **25**, 135 (2000).

[10]B. Chen, R. A. Dilanian, S. Teichmann, B. Abbey, A. G. Peele, G. J. Williams, P. Hannaford, L. V. Dao, H. M. Quiney, and K. A. Nugent, Phys. Rev. A **79**, 023809 (2009).
[11]M. Lewenstein, P. Balcou, M. Y. Ivanov, A. L'Huillier, and P. B. Corkum, Phys. Rev. A **49**, 2117 (1994).
[12]O. Smirnova, Y. Mairesse, S. Patchkovskii, N. Dudovich, D. Villeneuve, P. Corkum, and M. Yu. Ivanov, Nature **460**, 972 (2009).
[13]H. J. Worner, J. B. Bertrand, D. V. Kartashov, P. B. Corkum, and D. M. Villeneuve, Nature **466**, 604 (2010).
[14]S. Teichmann, B. Chen, R. A. Dilanian, P. Hannaford, and L. V. Dao, J. Phys. D: Appl. Phys. **42**, 135108 (2009).
[15]U. Eichmann, T. Nubbemeyer, H. Rottke, and W. Sandner, Nature **461**, 1261 (2009).
[16]E. Gloaguen, J. M. Mestdagh, L. Poisson, J. P. Visticot, and B. Soep, AIP Conf. Proc. **762**, 869 (2005).
[17]A. D. Shiner, B. E. Schmidt, C. Trallero-Herrero, P. B. Corkum, J.-C. Kieffer, F. Legare, and D. M. Villeneuve, J. Phys. B **45**, 074010 (2012).
[18]P. Balcou, P. Salieres, A. L'Huillier, and M. Lewenstein, Phys. Rev. A **55**, 3204 (1997).
[19]E. Constant, D. Garzella, P. Breger, E. Mével, Ch. Dorrer, C. Le Blanc, F. Salin, and P. Agostini, Phys. Rev. Lett. **82**, 1668 (1999).
[20]E. Mevel, E. Constant, D. Garzella, P. Breger, Ch. Dorrer, C. Le Blanc, F. Salin, and P. Agostini, AIP Conf. Proc. **525**, 373 (2000).
[21]C. Winterfeldt, C. Spielmann, and G. Gerber, Rev. Mod. Phys. **80**, 117 (2008).
[22]G. Vitrant, J. M. Raimond, M. Gross, and S. Haroche, J. Phys. B **15**, L49 (1982).
[23]A. Zair, M. Holler, A. Guandalini, F. Schapper, J. Biegert, L. Gallmann, U. Keller, A. S. Wyatt, A. Monmayrant, I. A. Walmsley, E. Cormier, T. Auguste, J. P. Caumes, and P. Salieres, Phys. Rev. Lett. **100**, 143902 (2008).
[24]N. Dudovich, J. L. Tate, Y. Mairesse, D. M. Villeneuve, P. B. Corkum, and M. B. Gaarde, Phys. Rev. A **80**, 011806 (R) (2009).
[25]H. Lefedve-Brion and R. W. Field, *The Spectra and Dynamics of Diatomic Molecules* (Elsevier, Amsterdam, 2004).
[26]M. Wollenhaupt, A. Assion, D. Liese, Ch. Sarpe-Tudoran, T. Baumert, S. Zamith, M. A. Bouchene, B. Girard, A. Flettner, U. Weichmann, and G. Gerber, Phys. Rev. Lett. **89**, 173001 (2002).